

Responses to Referee's comments

We are grateful to the reviewers for their valuable and helpful comments on our manuscript “**Mechanistic insights into marine boundary layer nucleation: synergistic interactions of typical sulfur, iodine, and nitrogen precursors**” (MS No.: egosphere-2025-5622). We have revised the manuscript carefully according to reviewers' comments. The point-to-point responses to the Referee's comments are summarized below:

Jing Li and coworkers have responded to our concerns and significant improvements have been made to the revised manuscript. A lot of the discussion in the response letter is very valuable to the present study, so we would like the authors to add more of the comments in the response letter explicitly to the manuscript. Hence, we believe that a minor further revision is needed before publication. Our remaining concerns are outlined below:

Response: We thank the reviewer for the professional comments, which have significantly improved the manuscript. We also appreciate the editor for providing us with the opportunity to further refine the paper, and the reviewer's efforts in re-evaluating our work and providing valuable comments and positive feedback.

SOC: The authors did not entirely address our concern regarding this point. Spin-orbit TD-DFT is, as far as we are aware, not implemented in Gaussian16. There are some third-party programs that can take the output of a Gaussian TD-DFT calculation and calculate the spin-orbit coupling. Furthermore, the dhf-TZVP-2c is a basis set only implemented in ORCA. Thus, we are in doubt about how you have performed these calculations. Please elaborate how exactly these calculations were carried out and do this explicitly in the manuscript. And a further correction on your statement on the results in Engsvang et al., it stabilizes at a maximum of 0.3 kcal/mol for the pure HIO_3 – HIO_3 interaction.

Response: We apologize for not accurately understanding your comment initially, which caused confusion in our response.

Response to the SOC and basis set issue:

As correctly pointed out, spin-orbit TD-DFT is not implemented in Gaussian 16. In our

study, the spin-orbit effect was evaluated by two-component spin-orbit DFT (SO-DFT) single-point calculations, rather than spin-orbit TD-DFT for excited states. To perform the SO-DFT calculations in Gaussian 16, the dhf-TZVP-2c basis sets compatible with two-component relativistic treatments was employed here. Meanwhile, the keyword of the employed functional was specified with the prefix “g” (e.g., *g*ωB97X-D). For the energy calculations, the effect of spin-orbit coupling (SOC) was estimated as the difference between the single-point energies obtained from SO-DFT and conventional DFT calculations on the same geometry.

Regarding the basis set, the reviewer is correct that dhf-TZVP-2c is not a standard built-in Gaussian basis set and is native to the ORCA program. In our calculations, this basis set was supplied manually in Gaussian 16 through the general basis-set input (*genecp*) format. The basis-set definition was taken from the Turbomole basis-set library (<https://basissets.turbomole.org/>), which provides the corresponding basis information.

An example in the Gaussian 16 installation directory, *test1198*, demonstrates the use of a two-component pseudopotential at the HF level for calculations on the Sg atom.

Correction regarding Engsvang et al.:

We thank the reviewer for this precise correction. After carefully re-examining the work of Engsvang et al. (2024), we confirm that the stabilization energy for the pure HIO₃–HIO₃ interaction reaches a maximum of 0.3 kcal mol⁻¹. The value in the original manuscript has been corrected.

Electronic Energies: Errors below 1 kcal/mol are usually said to be within chemical accuracy. If you have an error larger than this in the binding energy, you expect an error in the formation rate of at least an order of magnitude. This is based on the calculation of the evaporation rate (Ortega et al. 2012), where the binding free energy of the cluster is used in the exponential. How is this congruent with an error of 1.68 kcal/mol on for example the IA–DMA. Would that not indicate a significant overestimation of the formation rate? Could this not explain why it is only the lower bounds of your later results that overlap with the actual observations? Would it not also “leave room” for all the other nucleation pathways / stabilizing effects (ionization,

hydration) that would be present in reality? Furthermore, the findings in Table R1 should be added to the manuscript or supplementary information.

Furthermore, we suggest that you tone down the argument about good agreement with observations. The agreement is because you are looking at a limited model system. Refining that system to the highest degree of accuracy will obviously result in predictions that are equal to or below the actual measurements. This is due to all the other factors that could also contribute, because very rarely experiments are set up to isolate a single nucleation mechanism (even if they try to interpret it as such). Thus, if you are overestimating the formation rate with a subset of the nucleation, you would greatly overestimate it with the whole.

Response: Thank you for your insightful comments. Indeed, if we take the ZORA-CCSD(T)/TZVPP level of theory used in Engsvang et al. (2024) as the reference “gold standard”, our calculated binding energy for $(\text{IA})_1(\text{DMA})_1$ dimer is overestimated by $1.68 \text{ kcal mol}^{-1}$, which exceeds the conventional chemistry accuracy threshold of 1 kcal mol^{-1} . However, our comparison also reveals that the binding energy for $(\text{IA})_1(\text{MSA})_1$ is overestimated by only $0.17 \text{ kcal mol}^{-1}$, while that for $(\text{IA})_1(\text{MSA})_1(\text{DMA})_1$ is underestimated by $0.98 \text{ kcal mol}^{-1}$. Although larger clusters were not benchmarked due to the high computational cost of the ZORA-CCSD(T) calculations (Lesiuk, 2022; Khatun et al., 2023), these available results suggest a cluster-dependent error pattern rather than a consistent bias toward over-stabilization of the entire IA–MSA–DMA pathway. Moreover, Schmitz and Elm (2020) showed that the DLPNO-CCSD(T)/aug-cc-pVTZ(-PP) level of theory employed in our work can yield both overestimations and underestimations, but still produces RMSD values within 1 kcal mol^{-1} for the tested cluster formation energies, thereby supporting the overall accuracy of this method. In addition, this level of theory has been successfully applied in other studies of iodine-containing nucleation systems (Ma et al., 2023; He et al., 2023).

To further assess whether the $1.68 \text{ kcal mol}^{-1}$ overestimation in the $(\text{IA})_1(\text{DMA})_1$ cluster binding energy could substantially bias the predicted nucleation rates, we performed an additional sensitivity analysis by correcting the energies of the three benchmarked clusters relative to our original results and recalculating the corresponding formation rates. The results show that although such energy corrections can substantially affect individual evaporation rates,

for instance by changing the $(\text{IA})_1(\text{DMA})_1$ cluster evaporation rate by about one order of magnitude, the overall nucleation rate is affected to a much smaller extent (Fig. S9). This behavior likely reflects partial error cancellation, since the benchmark tests indicate both overestimations and underestimations for different clusters rather than a uniform systematic bias.

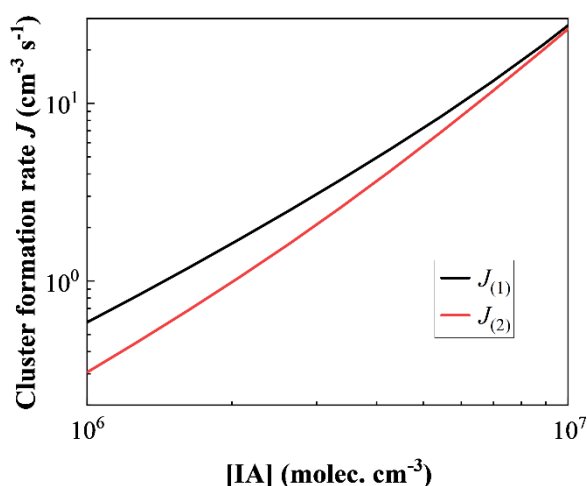


Figure S9. Cluster formation rates of the IA–MSA–DMA system under different energy conditions. Common conditions: $T = 278$ K, $CS = 2.0 \times 10^{-3} \text{ s}^{-1}$, $[\text{IA}] = 10^6 - 10^7 \text{ molec. cm}^{-3}$, $[\text{MSA}] = 10^7 \text{ molec. cm}^{-3}$, and $[\text{DMA}] = 0.25 \text{ pptv}$. $J_{(1)}$ represents the baseline formation rate using our original calculated Gibbs free energies. $J_{(2)}$ tests the sensitivity by applying the following energy corrections: $+1.68 \text{ kcal mol}^{-1}$ to the $(\text{IA})_1(\text{DMA})_1$ cluster, $+0.17 \text{ kcal mol}^{-1}$ to the $(\text{IA})_1(\text{MSA})_1$ cluster, and $-0.98 \text{ kcal mol}^{-1}$ to the $(\text{IA})_1(\text{MSA})_1(\text{DMA})_1$ cluster.

As suggested, we have added the data of Table R1 (now Table S5) in the Supporting Information. We have also added the following discussion in the revised Supporting Information:

“To assess the accuracy of our computational protocol, we performed benchmark tests against higher-level theoretical methods. Taking the ZORA-CCSD(T)/TZVPP level of theory used in Engsvang et al. (2024) as the reference, our calculated binding energies show varying deviations depending on the cluster composition (Table S5). For the $(\text{IA})_1(\text{DMA})_1$ dimer, the deviation reaches $1.68 \text{ kcal mol}^{-1}$, which exceeds the conventional threshold for chemical accuracy (1 kcal mol^{-1}). However, the benchmark tests also reveal that the binding energy for

(IA)₁(MSA)₁ is overestimated by only 0.17 kcal mol⁻¹, while that for (IA)₁(MSA)₁(DMA)₁ is actually underestimated by 0.98 kcal mol⁻¹. Although larger clusters were not benchmarked due to the high computational cost of the ZORA-CCSD(T) calculations (Lesiuk, 2022; Khatun et al., 2023), these available results suggest a cluster-dependent error pattern rather than a consistent bias toward over-stabilization of the entire IA–MSA–DMA pathway. Moreover, Schmitz and Elm (2020) showed that the DLPNO-CCSD(T)/aug-cc-pVTZ(-PP) level of theory employed in our work can yield both overestimations and underestimations, but still produces RMSD values within 1 kcal mol⁻¹ for the tested cluster formation energies, thereby supporting the overall accuracy of this method. In addition, this level of theory has been successfully applied in other studies of iodine-containing nucleation systems (Ma et al., 2023; He et al., 2023).

To further assess whether the 1.68 kcal mol⁻¹ overestimation in the (IA)₁(DMA)₁ cluster binding energy could substantially bias the predicted nucleation rates, we performed an additional sensitivity analysis by correcting the energies of the three benchmarked clusters relative to our original results and recalculating the corresponding formation rates. The results show that although such energy corrections can substantially affect individual evaporation rates, for instance by changing the (IA)₁(DMA)₁ cluster evaporation rate by about one order of magnitude, the overall nucleation rate is affected to a much smaller extent (Fig. S9). This behavior likely reflects partial error cancellation, since the benchmark tests indicate both overestimations and underestimations for different clusters rather than a uniform systematic bias.”

Finally, we agree that the apparent agreement between modeled and observed formation rates should be interpreted with caution, because the present simulations focus on a limited nucleation subsystem. Accordingly, we have toned down the discussion of the agreement with observations to more explicitly highlight the limitations of this study. The revisions are as follows:

Page 14, line 333: “bringing them into closer alignment with the observed nucleation rate range” is revised to “bringing them into the range of the observed nucleation rates”.

Page 14, line 337: “ternary nucleation driven by synergistic effects can effectively capture the

observed nucleation rates” is revised to “ternary nucleation driven by synergistic effects can produce formation rates comparable to those observed”.

Page 14, line 339: *“the MSA-enhanced ternary nucleation appears capable of reproducing the nucleation rates observed at Marambio” is revised to “the MSA-enhanced ternary nucleation yields rates that partially fall within the range observed at Marambio”.*

Page 15, lines 373-376: *“Mechanistic analysis indicates that the IA–MSA–DMA ternary nucleation is most evident under cold, sulfur- and nitrogen-rich conditions, and the simulated rates under polar-site conditions (Marambio) align well with field observations, advancing our understanding of NPF events.” is revised to “Mechanistic analysis indicates that the IA–MSA–DMA ternary nucleation can be evident under cold, sulfur- and nitrogen-rich conditions, and the simulated rates under polar-site conditions (Marambio) are partially comparable to the range of field observations, providing insights into the potential role of this mechanism in observed NPF events.”*

In summary, the reviewer has indeed provided a more comprehensive and overarching perspective, raising many important factors that need to be considered when comparing simulations with observations. This is extremely critical for improving the manuscript.

The Cluster Formation Rate:

Limited cluster size: We do acknowledge that your largest clusters could be past the critical cluster size. But the exact location of the critical point will depend on the binding strength of the gasses involved. Furthermore, you set out to predict the formation rate (usually reported at 1.5 nm), during the process of growing from the 1.2 nm cluster up to the 1.5 nm, clusters may be lost due to for example coagulation processes. Thus, the number, you report will still be an overestimation due to the losses incurred before they are measured. You cite a passage from Kubečka et al., however, we believe that you might have miscited the text. The context of the passage is valid in the low temperature, high concentration regime, where SA–EDA exhibits strong, stable nucleation. The full citation is *“Nevertheless, even for the SA–EDA system, a small drop in particle formation rate is observed when increasing simulation scheme size from*

3x3 to 4x4. Hence, an even larger simulation scheme with more postcritical clusters might be required to calculate the true J . This clearly indicates that, for most of the computational two-component NPF studies, the particle formation rate is overestimated at the given cluster stabilities.” The effect of increasing the size is larger if you are not in the high concentration regime, which is most likely not the case with trace gases in the Arctic. Generally, you could expect an order of magnitude drop, all depending on how the lower temperature of your site cancels out with the lower availability of gases. We suggest that you revise the passage you added to more adequately reflect the findings. Furthermore, we believe you should also add a section discussing the difference in your simulated formation rate and the nucleation rate reported due to the loss processes from 1.2 to 1.5 nm as pointed out above.

Response: We thank the reviewer for this insightful comment regarding the limitations associated with the cluster size of the simulation scheme and the potential loss processes between 1.2 and 1.5 nm. We agree that both factors can lead to an overestimation of the reported formation rates and therefore warrant careful discussion.

First, regarding the difference between simulated formation rates and experimentally reported nucleation rates, we note that particle formation rates are typically reported at a larger size (e.g., 1.5 nm), whereas our simulations track the formation of clusters at 1.2 nm. During the growth from 1.2 to 1.5 nm, clusters may be lost due to coagulation or scavenging by preexisting particles. According to the Kerminen–Kulmala equation (Kulmala et al., 2012), the relationship between formation rates at different sizes can be estimated by considering the growth rate and condensation sink, in which cluster formation rates for d_2 nm clusters (J_{d_2}) relate to those for larger diameter d_1 nm clusters (J_{d_1}) by

$$J_{d_1} = J_{d_2} \exp \left\{ \gamma \left(\frac{1}{d_1} - \frac{1}{d_2} \right) \frac{CS'}{GR_{d_1-d_2}} \right\} \quad (S4)$$

where the parameter γ depends on many factors but can usually be approximated by assuming it to be equal to $0.23 \text{ nm}^2 \text{ m}^2 \text{ h}^{-1}$. The $GR_{d_2-d_1}$ is the initial cluster growth rate from d_2 to d_1 nm, and CS' represents condensation sink of clusters by preexisting particles. GR was measured to be $3.2 - 4.4 \text{ nm} \cdot \text{h}^{-1}$ in the $1.1 - 2.0 \text{ nm}$ size range during three observed events (Xia et al., 2020; Yu et al., 2019). According to the study of Kerminen and Kulmalab (2002), we have converted

the CS value to CS' by the following equation (Kerminen and Kulmala, 2002):

$$CS = 4\pi D_i CS' \quad (S5)$$

where D_i is the diffusion coefficient of the condensing vapor, usually assumed to be sulfuric acid ($0.08 \text{ cm}^2 \text{ s}^{-1}$) (Kulmala et al., 2012).

At Marambio, the CS value is 0.00065 s^{-1} and the corresponding CS' value is about 6.5 m^{-2} . At Aboa, the CS value is 0.0004 s^{-1} and the CS' value is about 4.0 m^{-2} . Based on these values, the calculated $J_{1.5}$ is approximately 0.93 – 0.95 times $J_{1.2}$ at Marambio, and 0.95 – 0.97 times $J_{1.2}$ at Aboa. This reduction arises from the loss of clusters during their growth from 1.2 nm to 1.5 nm, mainly due to processes such as coagulation. Therefore, if the formation rate is not converted between these sizes, the reported rate may be slightly overestimated. The resulting small difference between $J_{1.2}$ and $J_{1.5}$ indicates that the loss during this short growth interval is likely limited under the considered conditions, which is similar to previous results from Xia et al. (2020). Now, we have added the aforementioned conversion relationship in the revised Supporting Information and included a discussion of this point in the revised manuscript to clarify that the simulated $J_{1.2}$ should not be directly equated to the measured $J_{1.5}$. The specific modification is located on Page 13, Lines 325-327, as follows:

“It should be noted that the field observation data presented here correspond to $J_{1.5}$, whereas our simulated values are $J_{1.2}$. Therefore, to enable a direct comparison, the simulated $J_{1.2}$ values were converted to $J_{1.5}$ according to Eq. S4.”

In addition, we fully agree with the reviewer's point that for the SA–EDA acid-base system under high-concentration conditions, increasing the simulation scheme size generally has a relatively small effect on the calculated formation rates, whereas outside the high-concentration regime the difference may become more pronounced, potentially reaching an order-of-magnitude decrease. To avoid any possible misunderstanding for readers, we have therefore removed the citation from the manuscript. Nevertheless, we note that Figure S4 of Kubečka et al. (2023) shows that for the SA–DMA–EDA ternary system the change in formation rate is less than one order of magnitude when the simulation scheme is expanded from 3×3 to 4×4 , which may provide a useful reference for evaluating the possible magnitude of rate

overestimation in the ternary IA–MSA–DMA system studied here.

SA vs. MSA: The results and the discussion in your response letter is very relevant, and we strongly recommend that you include this discussion in the revised manuscript as well.

Response: Thank you for your positive feedback. We have followed your suggestion and incorporated this discussion into the main text. Specifically, we have added the following text in the revised manuscript (page 9, lines 226-239):

“Furthermore, we compared the nucleation rates of the IA–SA–DMA and IA–MSA–DMA systems at 278 K and 248 K (Fig. S5). At 278 K, when the acid concentrations are equal ($[SA] = [MSA]$), the nucleation rate of the IA–SA–DMA system exceeds that of IA–MSA–DMA by 1–2 orders of magnitude, indicating that sulfuric-acid-driven nucleation is more efficient. This is consistent with sulfuric acid being a stronger nucleating precursor than MSA. However, the relative importance of these pathways in the real atmosphere also depends on the spatiotemporal distribution of their precursor concentrations. Over marine regions, the oxidation of DMS can produce both SO_2 (which is subsequently converted to SA) and MSA. Importantly, the DMS-to-MSA oxidation pathway is temperature dependent, with lower temperatures favoring MSA formation (Chen et al., 2023), potentially leading to enhanced atmospheric MSA accumulation. To reflect this realistic scenario, we compared the systems under colder conditions ($T = 248$ K). Under this temperature, when $[SA] = [MSA]$, the nucleation rate of the IA–MSA–DMA system remains significantly lower than that of the IA–SA–DMA system. However, when the MSA concentration is increased to $[MSA] = 5[SA]$ and $[MSA] = 10[SA]$, the nucleation rate of the IA–MSA–DMA pathway becomes higher. These results confirm that while the SA-driven pathway is effective, the IA–MSA–DMA mechanism we identified is potentially competitive, especially in cold environments where MSA production is enhanced. This underscores that MSA can be a co-dominant driver of iodine-mediated nucleation in specific marine regions.”

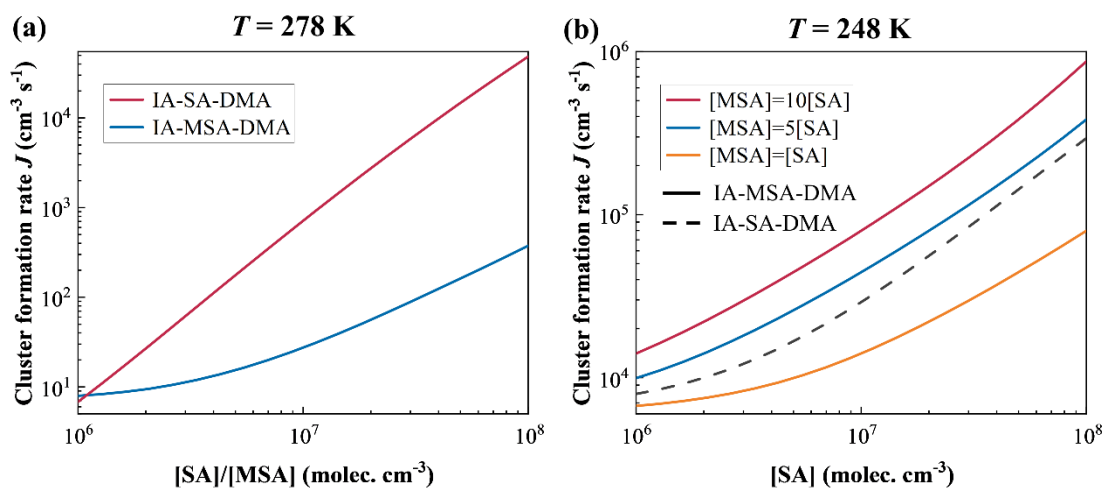


Figure S5. Cluster formation rates J ($\text{cm}^{-3} \text{s}^{-1}$) of the IA-SA-DMA and IA-MSA-DMA systems as a function of [SA] or [MSA] at (a) 278 and (b) 248 K. Key fixed conditions: $[\text{IA}] = 10^7 \text{ molec. cm}^{-3}$, $[\text{DMA}] = 0.25 \text{ pptv}$, $\text{CS} = 2.0 \times 10^{-3} \text{ s}^{-1}$.

Cluster Formation Pathway Section:

Line 234: We believe that we might have misunderstood each other here. As far as we understand the IA-DMA structures and energies are obtained from Ning et al. However, the point is that at [IA] above 10^7 cm^{-3} , you see a reduction of the ternary nucleation to the binary IA-DMA nucleation. Thus, at these concentrations the primary nucleation pathway follows the structures calculated in Ning et al. Therefore, your simulation reduces to that of Ning et al. above this threshold, revealing further complexity below this threshold. It would be good to explicitly state that this is an original finding in Ning et al and not in the present manuscript.

Response: Thanks for the helpful comments. We agree that at $[\text{IA}] > 10^7 \text{ cm}^{-3}$, the ternary IA-MSA-DMA nucleation effectively reduces to the binary IA-DMA pathway. In this [IA] regime, the dominant nucleation pathway therefore follows the mechanism previously identified in Ning et al. (2022). Following the reviewer's suggestion, we have revised the manuscript to explicitly clarify that the binary IA-DMA pathway originates from the work of Ning et al., while the present study mainly reveals the additional complexity of the nucleation mechanism at lower IA concentrations where MSA participates in the cluster formation process. The

revised sentence now reads:

“The dominant nucleation mechanism identified in the IA–MSA–DMA system involves two types of pathways: the ternary IA–MSA–DMA pathway and the binary IA–DMA pathway; notably, at high IA concentrations, the latter effectively reduces to the binary mechanism previously reported by Ning et al. (2022)”.

Comparison with Field Observations:

For Marambio: We believe that the expanded figure is a very good addition. However, in relation to the discussion added to this we have a few minor points:

1: HIO_3 varies over this expanded interval over the time periods considered in the Quéléver et al paper which is why we believe that the expanded figure is better. However, in their discussion of the relative contributions of the two mechanisms the authors do not consider concentration when nucleation events are observed. The lower bound of 10^4 molecules cm^{-3} is during the middle of the night. For the events shown in figure 4 of that paper, it varies from a maximum of around 10^6 molecules cm^{-3} down to around $2\text{--}3 \times 10^5$ molecules cm^{-3} , with a median of 3×10^5 molecules cm^{-3} during event days. Thus, from your figure 6, IA–DMA shouldn't, on its own, account for most of the nucleation?

Response: Thank you for your insightful comment regarding the IA concentration range during NPF events at Marambio. We have made a minor revision here: the condensation sink (CS) value used in our original simulations was a typical average value in polar regions (10^{-4} s^{-1}) (Baccarini et al., 2020). Upon re-examining Quéléver et al. (2022), we found the original CS value (10^{-4} s^{-1}) was not representative of the Marambio conditions. According their Table 1, we therefore updated the CS to the average value ($6.5 \times 10^{-4} \text{ s}^{-1}$), and correspondingly revised Figure 6.

The updated results show that at the median event-day IA concentration of 3×10^5 molec. cm^{-3} , the ternary IA–MSA–DMA mechanism can explain the observed nucleation rates. The binary IA–DMA pathway only begins to account for a small portion of the observations when IA concentrations exceed approximately 6×10^5 molec. cm^{-3} . The reviewer's suggestion to pay

closer attention to the IA concentration ranges during the two distinct NPF periods is particularly insightful, as it led us to consider a possible shift in the dominant nucleation mechanism. At low IA concentrations, MSA acts as an important supplementary precursor, facilitating ternary nucleation. As IA concentration increases, however, the relative contribution of MSA becomes less pronounced, while IA increasingly interacts with DMA and favors binary nucleation. Consequently, the binary pathway gradually becomes dominant and begins to account for the observed nucleation rates. We have incorporated this refinement into the revised manuscript and updated the corresponding discussion accordingly.

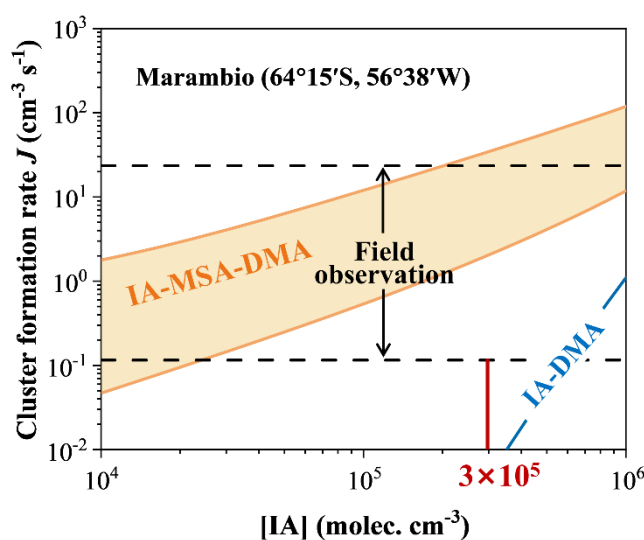


Figure 6. Comparison with the simulated cluster formation rate (J , $\text{cm}^{-3} \text{s}^{-1}$) and field observations under the ambient conditions of Marambio ($T = 273 \text{ K}$, $\text{CS} = 6.5 \times 10^{-4} \text{ s}^{-1}$, $[\text{IA}] = 10^4 - 10^6 \text{ molec. cm}^{-3}$, $[\text{MSA}] = 10^6 - 10^7 \text{ molec. cm}^{-3}$, and $[\text{DMA}] = 2.0 \text{ pptv}$).

2: Do not set “exceed or match” as the ultimate goal. You are looking at a simulated subsystem of the atmosphere, where you are only considering the contribution of IA, MSA, and DMA. What about the potential contribution from SA, which, as shown in fig. 4 and 5 of Quéléver et al. is also present? Could other bases such as AM not also add to this? We urge the authors to discuss this in the article (see for example the previous comment on the SA vs. MSA for parts of this). Likewise, we believe that you should discuss the effects of all the contributions that you have left out of your simulated system such as ions and water. Currently you match or

exceed with a relatively limited subset of the whole, which implies that you would wildly overestimate the nucleation rate if you also added SA, AM, or some of the many other things that could improve the chemical picture.

Response: We fully agree that the present simulations describe only a limited subsystem of the atmosphere, focusing specifically on the IA–MSA–DMA pathway. In the real atmosphere, additional species and processes can also contribute to cluster formation. For example, Quéléver et al. (2022) showed that sulfuric acid is present during NPF events at Marambio, and other bases such as ammonia may also participate in particle formation. In addition, ions and water vapor, which are not included in our simulations, can further stabilize molecular clusters.

Because our model considers only a subset of the atmospheric components, it should not be interpreted as a complete representation of the nucleation system. Rather, the IA–MSA–DMA mechanism investigated here represents one potential nucleation pathway that may contribute to particle formation under certain conditions. Following the reviewer’s suggestion, we have revised statements such as “match or exceed the observed nucleation rates” throughout the manuscript and clarified that the simulated rates should be interpreted within the context of this simplified subsystem. We have also added a discussion of the possible contributions from additional species (e.g., SA, ammonia, ions, and water) in the revised manuscript (pages 14-15, lines 350-357), which reads as follows:

“Moreover, our simulations only consider a limited subset of the atmospheric system, namely clusters containing IA, MSA, and DMA. In reality, additional species and processes may also affect particle formation. For example, Quéléver et al. (2022) showed that sulfuric acid is also observed during NPF events at Marambio, and ammonia can also participate in nucleation processes. In addition, ions and water vapor, which are not included in our model, may further influence cluster stability and formation. If all these factors were incorporated, the predicted formation rates would increase even further. Therefore, the simulated rates should be interpreted as the contribution from a specific IA-MSA-DMA nucleation pathway, rather than a complete description of Antarctic coastal NPF events. Future work should further consider the combined influence of other precursors.”

For Aboa: All experimental values reported in Xavier et al. are from Jokinen et al., figure 1c of Jokinen et al also only shows a single event day. In the supplement of Jokinen et al., fig S1A-F, they report the time-resolved simultaneous measurement of IA, MSA, and SA. The events marked in black are the events on which you base the experimental range. Based on some rough reading of the figures, we get that during events:

1: MSA is often around the lower end of your range: around $2\text{-}3 \times 10^6$ molecules cm^{-3} but did not observe any events with MSA below 2×10^6 molecules cm^{-3} , with a few events at $3\text{-}4 \times 10^6$ molecules cm^{-3} and another at $8\text{-}9 \times 10^6$ molecules cm^{-3} . Would this not indicate that we are more likely to be closer to the middle of your band, and thus more likely to exceed the observed nucleation?

Response: Thank you for your detailed comment regarding the MSA concentration range during NPF events at Aboa. In response, we have made two important refinements to our analysis:

First, we have updated the condensation sink (CS) value used in our simulations. Previously, we employed a typical average value of 10^{-4} s^{-1} in polar regions (Baccarini et al., 2020). Upon closer inspection, we have now adopted a CS value of $4 \times 10^{-4} \text{ s}^{-1}$ based on the work of Kyrö et al. (2013), which is more representative of the conditions at Aboa.

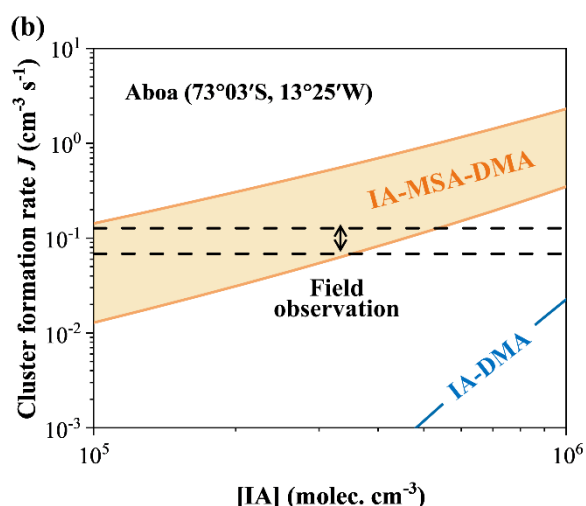


Figure 6(b). Comparison with the simulated cluster formation rate (J , $\text{cm}^{-3} \text{ s}^{-1}$) and field observations under the ambient conditions of Aboa ($T = 268 \text{ K}$, $\text{CS} = 4 \times 10^{-4} \text{ s}^{-1}$, $[\text{IA}] = 10^5 - 10^6 \text{ molec. cm}^{-3}$, $[\text{MSA}] = 2 \times 10^6 - 9 \times 10^6 \text{ molec. cm}^{-3}$, and $[\text{DMA}] = 0.055 \text{ pptv}$).

Second, we have carefully re-examined the source data in Jokinen et al. (Supporting Information, Figure S1A-F). Based on your observation, we have refined the MSA concentration range for our simulations to $2 \times 10^6 - 9 \times 10^6$ molec. cm^{-3} , which more accurately reflects the values observed during actual NPF events.

The updated results are presented in the revised Fig. 6(b). As shown, the formation rates for the binary IA–DMA pathway remain below the field observations across the entire IA concentration range. For the ternary IA–MSA–DMA mechanism, it yields higher rates. Although it may underestimate the field-observed nucleation rates under low-IA conditions, as the reviewer correctly noted, it also tends to overestimate the observations under part of the examined conditions.

2: IA is split between some events in the $3\text{-}5 \times 10^5$ molecules cm^{-3} range and some in the $7\text{-}9 \times 10^5$ molecules cm^{-3} range. With this, would we not have that it is split between the case where IA–DMA is irrelevant, and the case where it starts to account for a significant part of the nucleation?

Response: We thank the reviewer for this insightful observation regarding the distribution of IA concentrations during nucleation events at Aboa. Based on our updated simulations using the revised CS value ($4 \times 10^{-4} \text{ s}^{-1}$ from Kyrö et al. (2013)), we find that the binary IA–DMA pathway yields formation rates that remain substantially below the field observations across the entire IA concentration range ($10^5 - 10^6$ molec. cm^{-3}). This is consistent with the understanding that multiple nucleation precursors coexist in the real atmosphere and likely contribute collectively to the observed nucleation rates, rather than any single binary mechanism dominating under specific concentration range.

As the reviewer correctly noted, IA concentrations during NPF event days at Aboa are indeed split between a lower range ($3\text{-}5 \times 10^5$ molec. cm^{-3}) and a higher range ($7\text{-}9 \times 10^5$ molec. cm^{-3}). However, even at the higher end of this range, our updated results indicate that the IA–DMA pathway alone cannot account for a fraction of the observed nucleation. This further underscores the need for additional stabilizing species—such as MSA, SA, ammonia, ions, or water vapor—to explain the measured rates, and supports the role of the ternary IA–MSA–

DMA mechanism as a complementary pathway.

3: SA does not dip below 10^7 molecules cm^{-3} during events, and it is thus always more prevalent than MSA. How does this fit with the figure in your response showing the relative strength of IA–SA–DMA and IA–MSA–DMA?

Response: Thank you for this incisive observation. We fully acknowledge your point: as you correctly noted, during NPF events at Aboa, SA concentrations remain consistently above 10^7 molec. cm^{-3} , while MSA is generally lower. Given that SA forms more stable clusters with IA and DMA—as evidenced by the higher formation rates for IA–SA–DMA shown in Fig. S5—it is clear that SA-driven pathways should dominate under these conditions.

Based on this reasoning, we recognize that the IA–MSA–DMA ternary mechanism is unlikely to be a major contributor to the observed nucleation at Aboa and cannot adequately explain the field measurements. Consequently, we have removed Fig. 6(b) and its corresponding discussion from the revised manuscript to avoid any misinterpretation.

We appreciate your critical insight, which has helped us ensure that our conclusions remain consistent with the observational data and the known chemistry of the system.

Generally: Overall, we would like more discussion in the manuscript of how your mechanisms fit into a broader context of the other research that has taken place. This is still excellent work. If it turns out that the MSA-assisted nucleation is maybe only a minor part of the total nucleation, that is also very much a result worthy of publication.

Response: We thank the reviewer for this constructive and insightful comment. The reviewer's broad perspective on atmospheric nucleation processes is highly appreciated and has helped us better position our work within the wider research landscape. We agree that placing the IA–MSA–DMA mechanism within the broader context of atmospheric nucleation research helps clarify both its significance and its limitations.

Inspired by the reviewer's suggestion, we have added a new paragraph in the revised

manuscript (pages 15-16, lines 377-389) to discuss how the proposed MSA-assisted pathway relates to these well-established mechanisms, including sulfuric acid (SA)-driven nucleation.

“Although this work highlights the nucleation potential of the IA–MSA–DMA pathway, it does not imply that this mechanism dominates marine nucleation. Rather, our intention is to illustrate the potential synergy among representative marine iodine-, sulfur-, and nitrogen-containing precursors using IA, MSA, and DMA as a tractable model system. In reality, marine nucleation precursors extend far beyond this simplified combination. Sulfuric acid (SA) is widely recognized as a stronger nucleating sulfur-containing precursor than MSA, while iodine oxoacids such as HIO₂ can effectively stabilize HIO₃-containing clusters. Other nitrogen-containing bases, including methylamine, trimethylamine, and NH₃, may also contribute to enhancing nucleation, with their importance largely determined by their spatiotemporal distributions in marine environments. Although explicitly accounting for all these interacting species remains challenging, it is reasonable to expect that when they coexist, additional precursors such as SA and HIO₂ may substantially influence nucleation. In this context, MSA may act as a complementary nucleating acid that enhances SA-driven nucleation, as suggested in previous studies (e.g., Bork et al. (2014)). Therefore, the IA–MSA–DMA pathway proposed here likely represents only minor part of a broader multicomponent nucleation network in marine atmospheres, but identifying this MSA-assisted pathway helps reveal how iodine-, sulfur-, and nitrogen-containing precursors may jointly contribute to marine particle formation.”

Furthermore: In lines 328-334 in the revised manuscript, you still cite Xavier et al. for the Aboa measurements. All the experimental/field measurements are from Jokinen et al.. The work by Xavier et al. attempts to simulate these measurements.

Response: Thank you for pointing out this citation issue. We have carefully checked the references and confirm that the experimental measurements at Aboa were reported by Jokinen et al., while Xavier et al. performed model simulations based on these measurements. Following your suggestion, the citation of Xavier et al. has been replaced with Jokinen et al.

Reference:

- Baccarini, A., Karlsson, L., Dommen, J., Duplessis, P., Vullers, J., Brooks, I. M., Saiz-Lopez, A., Salter, M., Tjernstrom, M., Baltensperger, U., Zieger, P. and Schmale, J.: Frequent new particle formation over the high Arctic pack ice by enhanced iodine emissions, *Nat. Commun.*, 11, 4924, <http://doi.org/10.1038/s41467-020-18551-0>, 2020.
- Bork, N., Elm, J., Olenius, T. and Vehkamäki, H.: Methane sulfonic acid-enhanced formation of molecular clusters of sulfuric acid and dimethyl amine, *Atmos. Chem. Phys.*, 14, 12023–12030, <http://doi.org/10.5194/acp-14-12023-2014>, 2014.
- Chen, J., Lane, J. R., Bates, K. H. and Kjaergaard, H. G.: Atmospheric Gas-Phase Formation of Methanesulfonic Acid, *Environ. Sci. Technol.*, 57, 21168–21177, <http://doi.org/10.1021/acs.est.3c07120>, 2023.
- Engsvang, M., Wu, H. and Elm, J.: Iodine clusters in the atmosphere I: Computational benchmark and dimer formation of oxyacids and oxides, *ACS Omega*, 9, 31521–31532, <http://doi.org/10.1021/acsomega.4c01235>, 2024.
- He, X.-C., Simon, M., Iyer, S., Xie, H.-B., Rörup, B., Shen, J., Finkenzeller, H., Stolzenburg, D., Zhang, R., Baccarini, A., Tham, Y. J., Wang, M., Amanatidis, S., Piedchierro, A. A., Amorim, A., Baalbaki, R., Brasseur, Z., Caudillo, L., Chu, B., Dada, L., Duplissy, J., Haddad, I. E., Flagan, R. C., Granzin, M., Hansel, A., Heinritzi, M., Hofbauer, V., Jokinen, T., Kemppainen, D., Kong, W., Krechmer, J., Kürten, A., Lamkaddam, H., Lopez, B., Ma, F., Mahfouz, N. G. A., Makhmutov, V., Manninen, H. E., Marie, G., Marten, R., Massabò, D., Mauldin, R. L., Mentler, B., Onnela, A., Petäjä, T., Pfeifer, J., Philippov, M., Ranjithkumar, A., Rissanen, M. P., Schobesberger, S., Scholz, W., Schulze, B., Surdu, M., Thakur, R. C., Tomé, A., Wagner, A. C., Wang, D., Wang, Y., Weber, S. K., Welti, A., Winkler, P. M., Zauner-Wieczorek, M., Baltensperger, U., Curtius, J., Kurtén, T., Worsnop, D. R., Volkamer, R., Lehtipalo, K., Kirkby, J., Donahue, N. M., Sipilä, M. and Kulmala, M.: Iodine oxoacids enhance nucleation of sulfuric acid particles in the atmosphere, *Science*, 382, 1308–1314, <http://doi.org/10.1126/science.adh2526>, 2023.
- Kerminen, V.-M. and Kulmala, M.: Analytical formulae connecting the “real” and the “apparent” nucleation rate and the nuclei number concentration for atmospheric nucleation events, *J. Aerosol Sci.*, 33, 609–622, [http://doi.org/10.1016/s0021-8502\(01\)00194-x](http://doi.org/10.1016/s0021-8502(01)00194-x), 2002.
- Khatun, M., Paul, S., Roy, S., Dey, S. and Anoop, A.: Performance of Density Functionals and Semiempirical 3c Methods for Small Gold–Thiolate Clusters, *J. Phys. Chem. A*, 127, 2242–2257, <http://doi.org/10.1021/acs.jpca.2c07561>, 2023.
- Kubečka, J., Neeffes, I., Besel, V., Qiao, F., Xie, H.-B. and Elm, J.: Atmospheric Sulfuric Acid-Multi-Base New Particle Formation Revealed through Quantum Chemistry Enhanced by Machine Learning, *J. Phys. Chem. A*, 127, 2091–2103, <http://doi.org/10.1021/acs.jpca.3c00068>, 2023.
- Kulmala, M., Petäjä, T., Nieminen, T., Sipilä, M., Manninen, H. E., Lehtipalo, K., Dal Maso, M., Aalto, P. P., Junninen, H., Paasonen, P., Riipinen, I., Lehtinen, K. E. J., Laaksonen, A. and Kerminen, V.-M.: Measurement of the nucleation of atmospheric aerosol particles, *Nat. Protoc.*, 7, 1651–1667, <http://doi.org/10.1038/nprot.2012.091>, 2012.
- Kyrö, E. M., Kerminen, V. M., Virkkula, A., Dal Maso, M., Parshintsev, J., Ruiz-Jimenez, J., Forsström, L., Manninen, H. E., Riekkola, M. L., Heinonen, P. and Kulmala, M.: Antarctic new particle formation from continental biogenic precursors, *Atmospheric Chemistry and Physics*, 13, 3527–

- 3546, <http://doi.org/10.5194/acp-13-3527-2013>, 2013.
- Lesiuk, M.: Quintic-scaling rank-reduced coupled cluster theory with single and double excitations, *J. Chem. Phys.*, 156, 064103, <http://doi.org/10.1063/5.0071916>, 2022.
- Ma, F., Xie, H. B., Zhang, R., Su, L., Jiang, Q., Tang, W., Chen, J., Engsvang, M., Elm, J. and He, X. C.: Enhancement of atmospheric nucleation precursors on iodic acid-induced nucleation: Predictive model and mechanism, *Environ. Sci. Technol.*, 57, 6944–6954, <http://doi.org/10.1021/acs.est.3c01034>, 2023.
- Ning, A., Liu, L., Zhang, S., Yu, F., Du, L., Ge, M. and Zhang, X.: The critical role of dimethylamine in the rapid formation of iodic acid particles in marine areas, *npj Clim. Atmos. Sci.*, 5, 92, <http://doi.org/10.1038/s41612-022-00316-9>, 2022.
- Quéléver, L. L. J., Dada, L., Asmi, E., Lampilahti, J., Chan, T., Ferrara, J. E., Copes, G. E., Pérez-Fogwill, G., Barreira, L., Aurela, M., Worsnop, D. R., Jokinen, T. and Sipilä, M.: Investigation of new particle formation mechanisms and aerosol processes at Marambio Station, Antarctic Peninsula, *Atmos. Chem. Phys.*, 22, 8417–8437, <http://doi.org/10.5194/acp-22-8417-2022>, 2022.
- Schmitz, G. and Elm, J.: Assessment of the DLPNO binding energies of strongly noncovalent bonded atmospheric molecular clusters, *ACS Omega*, 5, 7601–7612, <http://doi.org/10.1021/acsomega.0c00436>, 2020.
- Xia, D., Chen, J., Yu, H., Xie, H. B., Wang, Y., Wang, Z., Xu, T. and Allen, D. T.: Formation Mechanisms of Iodine-Ammonia Clusters in Polluted Coastal Areas Unveiled by Thermodynamics and Kinetic Simulations, *Environ. Sci. Technol.*, 54, 9235–9242, <http://doi.org/10.1021/acs.est.9b07476>, 2020.
- Yu, H., Ren, L., Huang, X., Xie, M., He, J. and Xiao, H.: Iodine speciation and size distribution in ambient aerosols at a coastal new particle formation hotspot in China, *Atmos. Chem. Phys.*, 19, 4025–4039, <http://doi.org/10.5194/acp-19-4025-2019>, 2019.
- Zhang, R., Xie, H. B., Ma, F., Chen, J., Iyer, S., Simon, M., Heinritzi, M., Shen, J., Tham, Y. J., Kurtén, T., Worsnop, D. R., Kirkby, J., Curtius, J., Sipilä, M., Kulmala, M. and He, X. C.: Critical Role of Iodous Acid in Neutral Iodine Oxoacid Nucleation, *Environ. Sci. Technol.*, 56, 14166–14177, <http://doi.org/10.1021/acs.est.2c04328>, 2022.